The Simplified Exchange Approximation: A New Method for Radiative Transfer Calculations

STEPHEN B. FELS[1] AND M. DANIEL SCHWARZKOPF

Geophysical Fluid Dynamics Laboratory/NOAA, Princeton University, Princeton, N. J. 08540

(Manuscript received 20 January 1975, in revised form 31 March 1975)

ABSTRACT

A new scheme for the efficient calculation of longwave radiative heating rates is proposed. Its speed and accuracy make it attractive for use in large atmospheric circulation models.

The approximation suggested is

$$q \approx q^e - q^e_{\mathrm{CTS}} + q_{\mathrm{CTS}},$$

where q is the heating rate, q^e an "emissivity" heating rate calculated using the strong-line approximation and neglecting variation of line intensity with temperature, q^e_{CTS} the heating rate calculated using the cool-to-space approximation and the emissivity assumption, and q_{CTS} the heating rate calculated by the cool-to-space approximation.

Tests using a variety of soundings indicate that for both clear sky and cloudy cases the new approximation is substantially more accurate than either the emissivity or the cool-to-space approximations alone. Deviations from exact calculations are generally under 0.05 K day^{-1}. Errors in the calculated flux at the surface are also shown to be small especially with the inclusion of a "heat from ground" term in the approximation.

Some alternate schemes using similar approximations are presented and their utility discussed.

1. Introduction

The calculation of radiative heating rates in the lower part of the earth's atmosphere is peculiar in that the problem lies not so much in obtaining a closed, formal solution, as in the numerical evaluation of this formal solution. Put differently, whereas the problem may be considered solved mathematically once reduced to quadratures of known functions, these integrals are so complicated that their evaluation is enormously time-consuming in practice. Over the years many attempts have been made to find convenient parameterizations of the problem, in order to render the computations manageable. Especially valuable has been the concept of two-parameter path-scaling and the use of random band models (cf. Goody, 1964, especially Chaps. 4 and 6; Rodgers and Walshaw, 1966) which together have led to a straightforward and relatively accurate calculational scheme.

For routine use in all but the smallest general circulation models, however, even such highly parameterized models require a great deal of computation time. There are two obvious strategies for reducing this computational burden:

1) One may compute radiative heating rates relatively infrequently, for example, once or twice a model day (Smagorinsky *et al.*, 1965). The limitations of this approach are obvious but for some purposes (e.g., climatological studies) it may be acceptable.

2) One can attempt to simplify the radiative calculation still further (e.g., Mügge and Möller, 1932; Elsasser, 1942; Yamamoto, 1952; Rodgers, 1967; Sasamori, 1968, 1970; Gierasch and Goody, 1967). In so doing, care must be taken that the accuracy of the calculation is maintained at a tolerable level.[2]

The present work falls in the second class; we shall describe an algorithm whose speed approaches that of methods based on radiation charts and whose accuracy, relative to Rodgers and Walshaw in a variety of tests, is of the order 0.03 K day^{-1}. The next section is devoted to an explanation of the method while subsequent sections discuss numerical results and alternate schemes.

[1] Geophysical Fluid Dynamics Program: support provided through Geophysical Fluid Dynamics Laboratory/NOAA Grant E22-21-70(G).

[2] What accuracy is required is a complicated question. Fels and Kaplan (1975) show that the difference in the general circulation which results from the use of two very different radiation algorithms may be substantial, but further investigation is needed.

2. The algorithm

The formal solution of the radiative transfer equations for an atmosphere in local thermodynamic equilibrium is

$$\left.\begin{aligned} F_\nu^{\text{net}} &= B_\nu(T(0))\tau_\nu(0,p)+\int_0^{p(\text{ground})} \frac{\partial B_\nu}{\partial p'}\tau_\nu(p,p')dp' \\ \frac{\partial T}{\partial t} &= c_p^{-1}g\int_0^\infty \frac{\partial F_\nu^{\text{net}}}{\partial p}d\nu \end{aligned}\right\}, \quad (1)$$

where $F_\nu^{\text{net}}(p)$ is the monochromatic net upward flux, $B_\nu(T)$ the blackbody function, $\tau_\nu(p,p')$ the monochromatic transmission function between levels p and p', averaged over all slant paths,[3] c_p is the specific heat of dry air at constant pressure, and g the gravitational acceleration.

The only radiatively active gases of concern to us here are CO_2, O_3 and H_2O. The distribution of CO_2 is sufficiently uniform and constant to make pre-computation of accurate broad-band transmission functions a practical device (Fels and Kaplan, 1975). This is not true for O_3, whose concentration is variable. Fortunately, however, its effects in the troposphere are not important. In the troposphere, water vapor is the chief absorber, having measurable opacity throughout most of the infrared spectrum. Its distribution is highly variable in both space and time, which makes precomputation of transmission functions impossible. The importance and variability of water vapor thus demand the use of efficient and accurate parameterizations. In their 1966 paper, Rodgers and Walshaw showed that the Goody random model and the Curtis-Godson approximation could be used for water vapor to obtain a broad-band analogue of (1) which may be written:

$$\frac{\partial T}{\partial t}(p)=c_p^{-1}g\sum_n \frac{\partial F_n}{\partial p}, \quad (2a)$$

$$F_n(p)=\int_{\Delta\nu_n} F_\nu(p)d\nu = B_n(T(0))\tau_n(0,p) + \int_0^{p(\text{ground})} \frac{\partial B_n}{\partial p'}\tau_n(p,p')dp', \quad (2b)$$

$$\tau_n(p,p')=\exp\left\{\frac{-a_n\bar{m}_n(p,p')}{[1+b_n\bar{m}_n(p,p')/\bar{\phi}_n(p,p')]^{\frac{1}{2}}}\right\}, \quad (2c)$$

where

$$\bar{m}_n(p,p')=\int_p^{p'} \Phi_n(T(p''))dm'', \quad (2d)$$

$$\bar{\phi}_n(p,p')=\bar{m}_n^{-1}p_{\text{lab}}^{-1}\int_p^{p'} p''\Psi_n(T(p''))dm'', \quad (2e)$$

$$B_n(T)=\int_{\Delta\nu_n} B_\nu(T)d\nu. \quad (2f)$$

About 20 spectral bands are required; the width of the nth is $\Delta\nu_n$. The numbers a_n and b_n may be obtained directly from laboratory data for line widths and intensities at a standard pressure (p_{lab}) and temperature (260 K). The intensity scaling functions $\Phi_n(T)$ and $\Psi_n(T)$ represent corrections for the dependence of line intensity and width on temperature, and by definition are unity when T is the standard temperature. These may also be determined from laboratory data. The integrals defining $\bar{m}_n(p,p')$ are taken over the absorber mass m'' between pressure levels p' and p.

The finite-differencing of these equations is in general straightforward. Evidently, the function $\tau_n(p,p')$ will be replaced by a matrix $\tau_n(p_i,p_i')$ and each element in this matrix will depend on the corresponding elements of two ancillary matrices, $\bar{m}_n(p_i,p_i')$ and $\bar{\phi}_n(p_i,p_i')$, all of which must be computed for each spectral band. It is this which makes even these highly parameterized radiation calculations so time-consuming.

For the amounts of water vapor typically found in the troposphere, it has been observed (Rodgers and Walshaw, 1966; Man-Li Wu, private communication) that the strong-line approximation [i.e., the neglect of 1 as compared to $b_n\bar{m}_n/\bar{\phi}_n$ in Eq. (2c)] is often permissible. If, in addition, we can neglect the variation of line intensity with temperature (i.e., the deviations of Φ_n and Ψ_n from unity), we are led to an enormous simplification, for now τ_n is a function of only one variable, namely

$$u(p,p')\equiv\bar{m}(p,p')\bar{\phi}(p,p')=p_{\text{lab}}^{-1}\int_p^{p'} p''dm'', \quad (3)$$

which is independent of n, the band index. The flux now may be written as

$$F(p)=G_1(T(0),u(0,p))T^4(0) + \int_0^{p(\text{ground})} \frac{\partial T^4}{\partial p'}G_2(T(p'),u(p',p))dp', \quad (4)$$

where

$$\left.\begin{aligned} G_1(T,u) &= T^{-4}\sum_n B_n(T)\tau_n(u) \\ G_2(T,u) &= \tfrac{1}{4}T^{-3}\sum_n \frac{\partial B_n}{\partial T}\tau_n(u) \end{aligned}\right\}. \quad (5)$$

The functions G_1 and G_2 may be pretabulated and the remaining quadrature done very simply. Such simpli-

[3] In what follows, we shall use a diffusivity factor of 1.66 to approximate this averaging. The error so introduced is believed to be small (Rodgers and Walshaw).

fications have been the traditional starting point for chart methods, and do indeed lead to a great reduction in computation time.

Unfortunately, the errors generated by such approximations may be quite substantial (as will be shown in the next section), so that these "emissivity" calculations are not by themselves sufficiently accurate for many purposes.

It is now profitable to turn to a completely different approach, the "cool-to-space" approximation (Rodgers and Walshaw). For an isothermal atmosphere at temperature T, the cooling rate is, from Eq. (2)

$$\frac{\partial T}{\partial t}=c_p^{-1}g\sum_n B_n(T)\frac{\partial \tau_n}{\partial p}(0,p). \tag{6}$$

The "cool-to-space" (CTS) approximation simply consists of assuming that (6) may be used to calculate cooling rates at every height, even when T is not constant.

The simplicity of (6) as compared to (2) lies in the fact that cooling rates are local functions of temperature, and depend only on the absorber distribution above the point in question. Thus in finite-difference versions of (6), we do not need to calculate the entire matrix array $\tau_n(p_i,p_i')$ but only one column. For a model with a large number of levels in the vertical, this is an important simplification. Unfortunately, while the CTS approximation is fairly accurate under some circumstances, it fails miserably in others (again, we put off detailed comparisons until a later section).

Regardless of the accuracy of the CTS approximation, we may formally divide the total IR heating rate into a CTS part and an exchange term. Let us therefore define[4]

$$q_{\text{exact}}\equiv\frac{\partial T}{\partial t}\quad\text{[as calculated from Eq. (2)]}$$

$$q_{\text{CTS}}\equiv\frac{\partial T}{\partial t}\quad\text{[as calculated from Eq. (6)]}$$

$$q_{\text{exchange}}\equiv q_{\text{exact}}-q_{\text{CTS}}.$$

This partitioning is completely separate from the simplification used in emissivity calculations, so that we may divide the total emissivity heating rate q^e into CTS and exchange terms (denoted q^e_{CTS} and q^e_{exchange}), just as above. The reason for so doing lies in the fact that the differences between q^e_{CTS} and q_{CTS} are generally far greater than those between q^e_{exchange} and q_{exchange}. Another way of saying the same thing is that the exchange term is quite insensitive to the approximations used in going from (2) to (4). This seems to be due to two separate effects. First the CTS term is generally much larger than the exchange term, so that the same *fractional* error is less damaging in the latter than in the former. Beyond this, however, the fractional error in the exchange term is usually smaller than that in the CTS. This is probably because a mean temperature of 260 K (the standard temperature) is not too far wrong for the lower layers of the troposphere which dominate the exchange contribution, but may be quite bad for the CTS term. If one accepts this for the moment, it is easy to see that it leads to a convenient computation scheme.

By assumption,

$$q_{\text{exchange}}\sim q^e_{\text{exchange}},$$

so that

$$q\sim q^e_{\text{exchange}}+q_{\text{CTS}}.$$

But

$$q^e_{\text{exchange}}\equiv q^e-q^e_{\text{CTS}},$$

or

$$q\sim q^e-q^e_{\text{CTS}}+q_{\text{CTS}}=q_{\text{approx}}. \tag{7}$$

This is, in fact, the new approximation which we propose as a useful and accurate computational tool. While its precision will be discussed subsequently, it is easy to see why it can lead to a very significant reduction in computation time.

The first term on the right-hand side of (7) is just the "emissivity" heating rate; we have already discussed the ease with which this may be computed. The next term, q^e_{CTS}, is even simpler, being a one-band, local calculation. The final term, q_{CTS}, though requiring a multi-band calculation, is nonetheless fast because the transmission functions required form a vector, rather than a matrix. This advantage, of course, is more pronounced the larger the number of vertical levels in the model.

Our approximation may be simply described in words as follows: calculate the exchange term crudely, using emissivities, and the cool-to-space term accurately. Of course, we have as yet to convince the reader that this is indeed a good approximation; we attempt this task next.

3. Results

a. Heating rates

We have tested the approximation scheme by direct comparison of calculations based on Eq. (4), which we shall call the "exact" results, and calculations using Eq. (7). Certain relevant computational details are discussed in Appendix A. Of the large number of cases tested, we have chosen six as illustrations. The first three are based on climatological temperatures and mixing ratios for the tropical, mid-latitude and polar regions, while the next three are actual observed data for the three different zones. Specific sources for the data are presented in Appendix B, along with the pressure layers used.

[4] Use of the word "exact" to describe heating rates means only that they are based on Eq. (2).

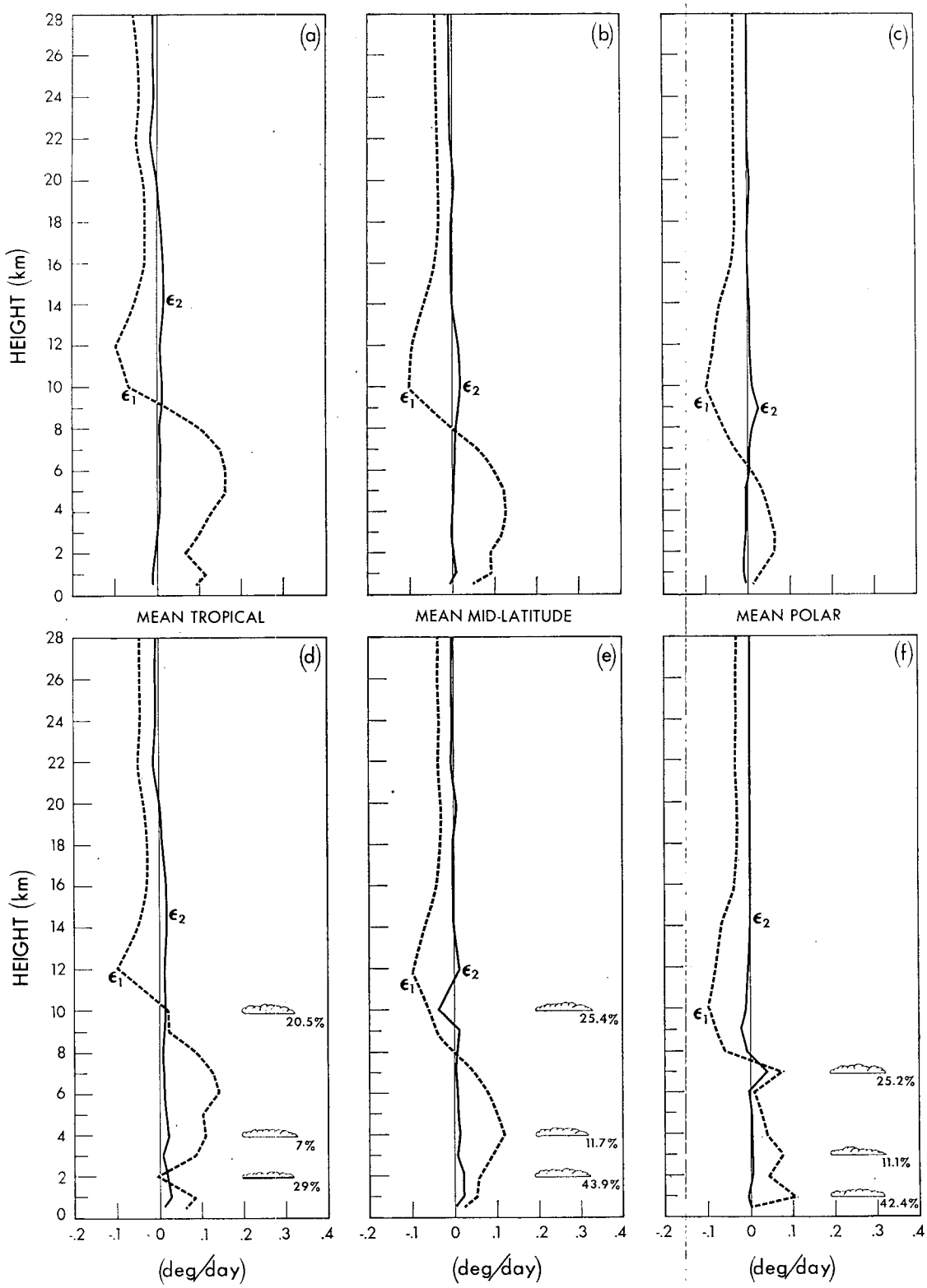

FIG. 1. Heating rate error curves for emissivity approximation ϵ_1 and CTS-corrected emissivity approximation ϵ_2. Parts (a)–(c) are for clear-sky conditions based on climatological mean data, while (d)–(f) are the same soundings but with clouds in the amounts and at the places shown. The tick marks on the vertical axis represent approximate data levels.

In every example we present graphs of two error quantities:

(i) $\epsilon_1 \equiv q^e - q_{\text{exact}}$

(ii) $\epsilon_2 \equiv q_{\text{approx}} - q_{\text{exact}}$

which, in general, are more instructive than the heating rates themselves. Figs. 1a, 1b and 1c show the errors for the mean climatological soundings under cloud-free conditions. The most obvious conclusion is that in general $|\epsilon_2|$ is much less than $|\epsilon_1|$; where this is not true $|\epsilon_1|$ itself is small. Thus the use of the CTS correction is remarkably successful in eliminating the errors due to the emissivity approximation.

In the tropical case, the largest value of $|\epsilon_2|$ is 0.016 K day^{-1}, as opposed to 0.16 K day^{-1} for $|\epsilon_1|$. In the mid-latitude and polar cases, the improvement due to the use of the CTS correction is almost as large, the worst value of $|\epsilon_2|$ being 0.025 K day^{-1} at 9 km in the polar case.

The smallness of $|\epsilon_2|$ in all three cases shows that the error in the emissivity approximation occurs almost completely in the CTS term, as indicated previously. This makes it relatively simple to understand the general features of the ϵ_1 curves, as is discussed in Appendix C.

Having seen that in the clear-sky cases our new approximation works very well, we turn to the cloudy case. To the extent that they may be treated as black radiators, there is no difficulty in incorporating clouds in the "exact" formulation (Manabe and Strickler, 1964). Their effect on our approximation scheme requires a separate investigation.[5]

Figs. 1d, 1e and 1f are similar to 1a, 1b and 1c, respectively, only differing by the presence of clouds in the amounts and at the levels shown. In all cases there is a slight but noticeable deterioration in accuracy relative to the clear-sky case. In the tropics, the largest value of $|\epsilon_2|$ is now 0.025 K day^{-1} and in the mid-latitude and polar cases, 0.04 K day^{-1}. The largest error occurs at the high cloud layer.

At first glance, it may seem surprising that the approximation remains good under these conditions, for beneath a completely overcast layer, q_{CTS} and q^e_{CTS} of Eq. (7) are both zero, so that there is no correction to the exchange term calculated using emissivities. In the cases chosen here, however, as in most realistic cases, the layers with high fractional cloud cover are near the ground; hence the temperature of the atmosphere beneath the clouds does not differ greatly from that of the clouds. Therefore the exchange term is itself relatively small, and errors in its calculation are proportionally less serious. This effect is illustrated clearly in the lowest two layers of Figs. 1b and 1e; notice that

[5] Clouds are incorporated into all terms (including the CTS term) by multiplying $\tau(p_i,p_j)$ by $1-c(p_i,p_j)$, where $c(p_i,p_j)$ is the fraction of horizontal area covered by clouds between levels p_i and p_j.

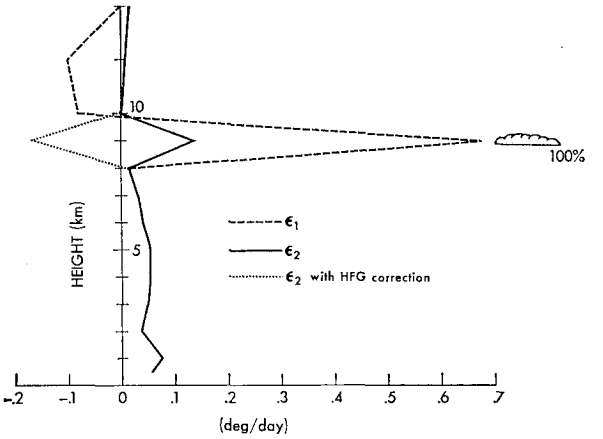

FIG. 2. Error curves for the mean tropical case with 100% cloud at 9 km. The line labeled "with HFG correction" is calculated using Eq. (14) of Section 3.

$|\epsilon_1|$ decreases substantially in this region, due to the presence of clouds.

Even in the extreme case of total overcast (with fully black clouds) at 9 km, the results are quite acceptable, as Fig. 2 indicates. The uncorrected error of 0.69 K day^{-1} at the cloud layer is reduced to 0.12 K day^{-1} by use of the CTS correction term. The humidity and temperature profiles are those of the mean tropical case. (The significance of the curve labeled "with HFG correction" will be explained subsequently.)

Figs. 3a–3f are similar to 1a–1f, except for the use of observed and therefore less smooth soundings. In the cloudless cases, the approximation again does very well in the troposphere, the worst errors being about 0.025 K day^{-1}. Errors using the uncorrected emissivity approximation for these layers range from 0.2 K day^{-1} in the tropics to 0.17 K day^{-1} in the mid-latitudes, so that again we achieve a very substantial improvement. At about 26 km in the tropical case, however, ϵ_1 reaches a value of -0.310 K day^{-1}; this is due to a distinct peak in the mixing ratio at that level leading to especially strong cooling, and a correspondingly large error using uncorrected emissivities. This deviation is reduced to -0.091 K day^{-1} by the use of the cool-to-space correction. The relatively large residual indicates that in this case, exchange terms are more important than in the previous cases.

It is appropriate to remark here on the accuracy of the CTS approximation (as opposed to the CTS correction). While in certain cases the CTS term alone gives a good estimate of the total cooling rate, this is emphatically not true in the presence of clouds (Man-Li Wu, private communication). In Fig. 4, we plot the error in the water vapor heating rates using the CTS approximation for the Trinidad data of Figs. 3a and 3d. In the clear-sky case the errors are already as large as 0.59 K day^{-1}; the deviation at the high cloud level is 3.48 K day^{-1}. These errors are far larger than those which

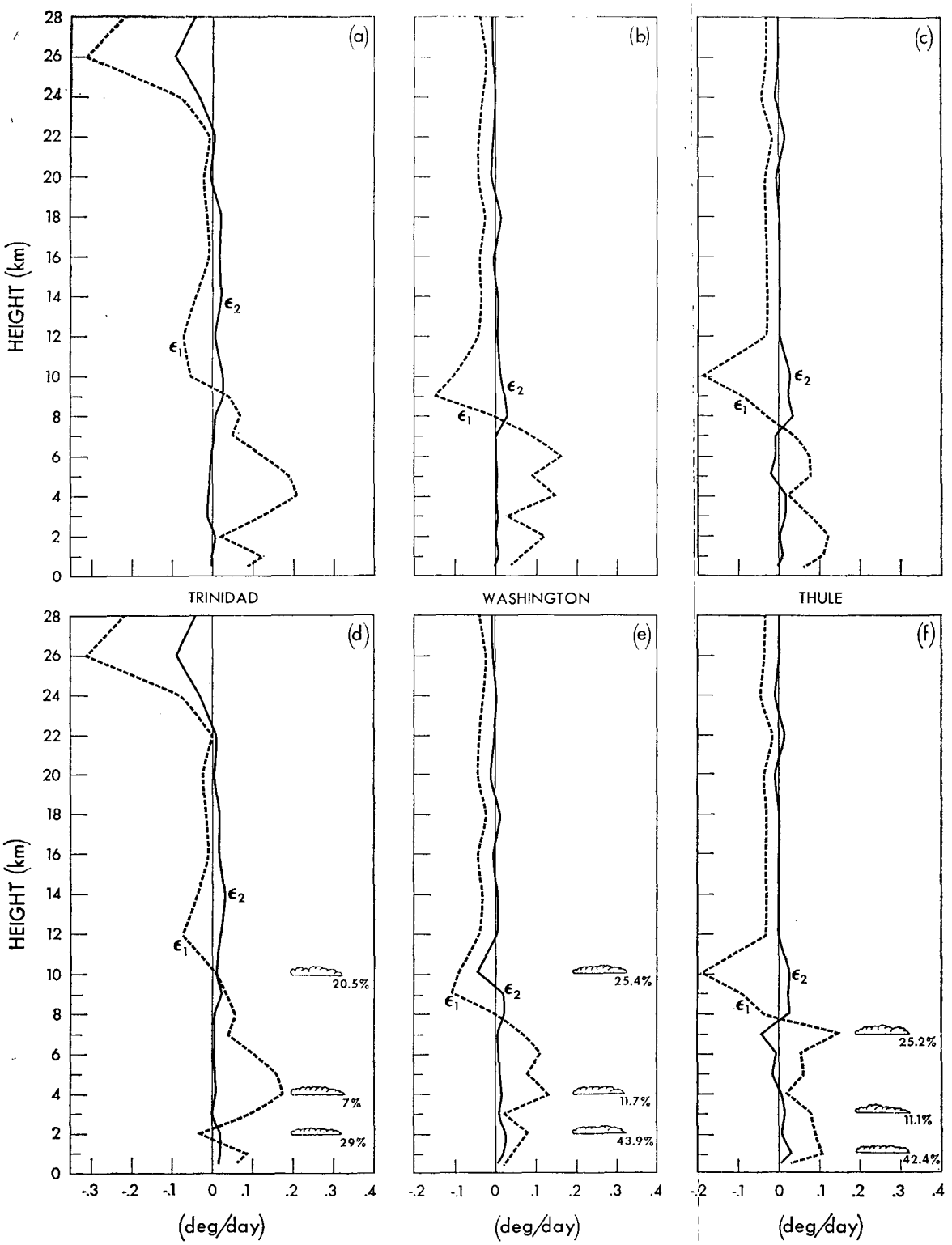

FIG. 3. As in Fig. 1 except for mixing ratios and temperatures based on observed data (see Appendix B).

exist in an uncorrected emissivity calculation, and for this reason we shall discuss the pure CTS approximation no further.

We may summarize the results of all cases tested (including several not discussed here) by saying that the CTS correction reduces the cooling rate errors very

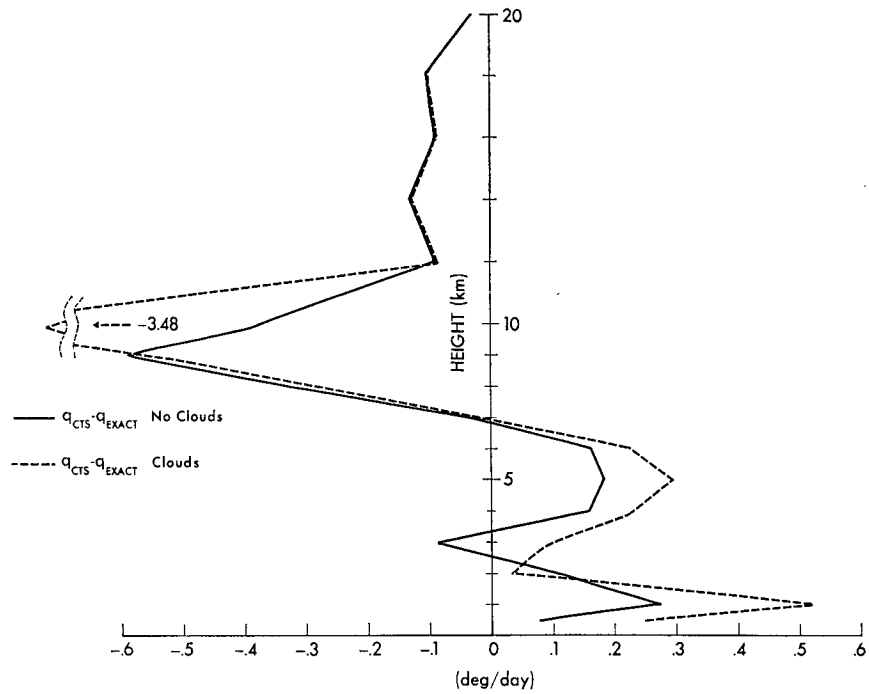

FIG. 4. Accuracy of the CTS approximation with and without clouds for the Trinidad sounding of Fig. 1.

substantially, especially in those places where the error is large. In Table 1, we show the rms values for ϵ_1 and ϵ_2 for each of the six cases discussed as a convenient recapitulation of our results.

b. *Calculation of flux at the ground*

In many applications, the surface temperature is determined by means of an assumed energy balance at the ground. This requires that we calculate the long-wave flux there.[6] It is important to notice that in calculating the "exact" CTS term, we have computed all the transmission functions necessary for a precise evaluation of the outgoing IR flux at the top of the atmosphere, since

$$F_n(0)=B_n(T(0))+\int_0^{p(\text{ground})}\frac{\partial B_n}{\partial p'}\tau_n(0,p')dp'. \quad (8)$$

By definition, if q_n is the exact heating rate for interval n, then

$$F_n(g)-F_n(0)=c_pg^{-1}\int_0^{p(\text{ground})}q_ndp'$$

or

$$F_n(g)=B_n(T(0))\times\int_0^{p(\text{ground})}\left[c_pg^{-1}q_n+\frac{\partial B_n}{\partial p'}\tau_n(0,p')\right]dp'. \quad (9)$$

Using our approximation,

$$q_n=q_n^e+q_{n\,\text{CTS}}-q_{n\,\text{CTS}}^e$$

$$=\frac{dF_n^e}{dp}+B_n(p)\frac{d}{dp}[\tau_n(0,p)-\tau_n^e(0,p)], \quad (10)$$

TABLE 1. Root mean square heating rate errors (K day^{-1}) for the 12 cases discussed in Section 3. C. and N.C. stand for clouds and no clouds.

	Mean tropical		Mean mid-latitude		Mean polar	
	N.C.	C.	N.C.	C.	N.C.	C.
rms ϵ_1	0.092	0.073	0.076	0.062	0.051	0.057
rms ϵ_2	0.009	0.014	0.007	0.013	0.007	0.011
	Trinidad		Washington		Thule	
	N.C.	C.	N.C.	C.	N.C.	C.
rms ϵ_1	0.122	0.111	0.078	0.063	0.061	0.073
rms ϵ_2	0.026	0.027	0.010	0.015	0.014	0.016

[6] A convenient order of magnitude estimate of the result of a flux error may be obtained by assuming that the fluxes at the surface are purely radiative:

$$\sigma T^4=F_{\text{SOLAR}}+F_{\text{IR}}$$
$$\Delta T=\Delta F_{\text{IR}}/4\sigma T^3$$

If $T=280$ K, $\Delta T=2\times10^{-1}\,\Delta F$. An error of 1 W m^{-2} will result in a temperature error of about 0.2°C.

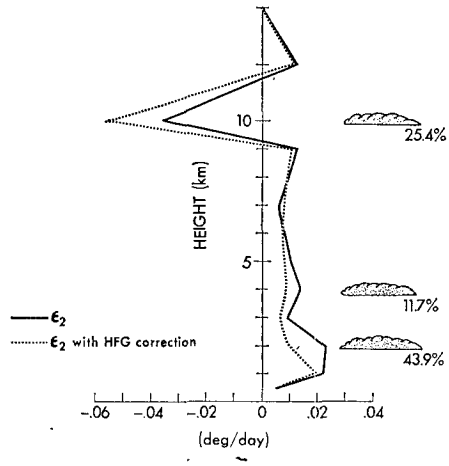

FIG. 5. Effect of the heat-from-ground correction. ϵ_2 is defined as previously, and is calculated with and without the HFG term. The sounding is that of Fig. 1e.

so that

$$F_n(g)\approx F_n^e(g)+\Big\{B_n(T(0))-F_n^e(0)+\int_0^{p(\text{ground})}\Big[B_n(p')\frac{d}{dp'}[\tau_n(0,p')-\tau_n^e(0,p')]+\frac{\partial B_n}{\partial p'}\tau_n(0,p')\Big]dp'\Big\}. \quad (11)$$

Here τ_n^e is the random model transmission function calculated in the strong-line limit, ignoring temperature variation of line intensities.

The term $F_n^e(g)$ is, of course, the emissivity value of the net flux at the ground, and the term in braces in Eq. (11) represents a correction thereto. By a simple integration by parts, this can be thrown into the computationally simpler form

$$F_n(g)\approx F_n^e(g)-B_n(g)[\tau_n(0,p_g)-\tau_n^e(0,p_g)]. \quad (12)$$

Before presenting the results of flux calculations based on this result, it is appropriate to discuss a refinement of our approximation scheme which in some cases is useful.

As the cool-to-space approximation considers only the photons lost to space by a layer, one can also include a term representing the photon exchange with the ground, or a "heat from ground" (HFG) term, (Feigel'son, 1970) which has the form

$$q_{\text{HFG}}=\sum_n [B_n(p)-B_n(p_g)]\frac{\partial\tau_n}{\partial p}(p,p_g). \quad (13)$$

In general, this is a small contribution to heating rates, since most of the water vapor is near the ground. We can, however, use this term in the same way as we do the CTS expression, to correct further the emissivity calculation, i.e.,

$$q\sim q^e+q_{\text{CTS}}-q^e_{\text{CTS}}+q_{\text{HFG}}-q^e_{\text{HFG}}. \quad (14)$$

The chief drawback here is that we now must calculate twice as many exact transmission functions as was previously necessary, a time-consuming process. If this is done, however, the calculated flux at the ground will be exactly correct, as can easily be shown.

A simple compromise between time and accuracy is to evaluate q_{HFG} crudely using the strong-line limit and an approximate temperature correction, assumed to be the same for all spectral intervals; with these assumptions q_{HFG} can be computed by a modified emissivity calculation. (Details are discussed in Appendix A.)

The manner in which this further correction modifies free atmospheric heating rates is interesting. It is clear that if the flux at both $p=0$ and the ground are correct, the pressure integral of the heating rate error over the atmosphere must be zero. Referring to Fig. 5, which in part recapitulates Fig. 1, we see that using the CTS correction alone, this is not the case. When the HFG term is included, the reduction in the error integral is achieved by a degradation in the accuracy of the approximation at the high cloud layer and an improvement in the lower troposphere, especially at the lower cloud layers.

Table 2 shows the ground flux errors for the six cases discussed previously, both with and without clouds. It is obvious that even without the use of the HFG term, the CTS correction makes a very substantial improvement in the calculated value of the ground flux. The agreement is best in the cloudless cases, as one would expect; the HFG correction is most useful in the cloudy cases where the residual errors are large.

c. The 10 μm continuum

We have as yet said nothing about the way in which the 10 μm continuum absorption region of water vapor is treated. If this absorption is parameterized as is done by Rodgers and Walshaw there is no problem as this term depends on the variable $u(p,p')$ defined in Eq. (3). There is evidence, however, that in the continuum region the absorber amount is scaled by the water vapor pressure, rather than the total pressure (Bignell, 1970), and that this can have an important effect on cooling rates calculated for tropical atmospheres (Cox, 1973). This "*e*-type" absorption can be incorporated, if necessary, by means of an ancillary emissivity table whose argument is the vapor pressure scaled absorber amount. It may, however, even be possible to use a simple total pressure scaled absorber amount in the exchange terms, and employ vapor pressure scaling in the CTS correction term.

d. Timing

Using our approximation, a 40-layer calculation requires about 0.1 s on an IBM 360–195 computer. An

TABLE 2. Errors in flux at ground (W m^{-2}) with and without HFG correction term for twelve cases discussed in Section 3. C. and N.C. stand for clouds and no clouds.

	Mean tropical		Mean mid-latitude		Mean polar	
	N.C.	C.	N.C.	C.	N.C.	C.
Exact-emissivity	−7.69	−5.39	−3.21	−1.97	−2.25	0.92
Exact-approximate	−0.65	−1.70	−0.56	−0.98	0.00	0.05
Exact-approximate with HFG correction	−0.45	−1.13	−0.35	−0.56	0.06	0.04
	Trinidad		Washington		Thule	
Exact-emissivity	−6.66	−4.62	−2.71	−1.67	−1.10	−0.84
Exact-approximate	−0.55	−1.41	−0.60	−0.88	−0.69	−0.71
Exact-approximate with HFG correction	−0.55	−1.01	−0.33	−0.46	−0.45	−0.49

exact calculation takes about 7 times as long. This ratio should be relatively independent of the machine used.

4. Alternate schemes

The insensitivity of the total heating rate to the value of the exchange term, which the results of the previous section demonstrate, lead us to consider an alternate approximation method, in which the exchange term is precalculated on the basis of "climatological" mixing ratios.[7] If this does give accurate answers, it would merely be necessary to calculate q_{CTS} anew for each temperature and humidity profile. This procedure would be more efficient than the method of the previous section, since the emissivity calculation of q_{exchange} requires a significant amount of time.

We made a modest test of this idea by applying it to 10 days of artificially generated mixing ratio data (cf. Appendix A for details). These mixing ratios were taken from a general circulation model history tape and have the advantage of providing a uniform set of time series for many different soundings.

The "climatic average" mixing ratios were obtained by simply averaging the mixing ratio for the first 5 days. This average mixing ratio profile [which we shall

[7] In so doing, there is no reason to employ an emissivity computation; we are here making a different type of approximation for q_{exchange}.

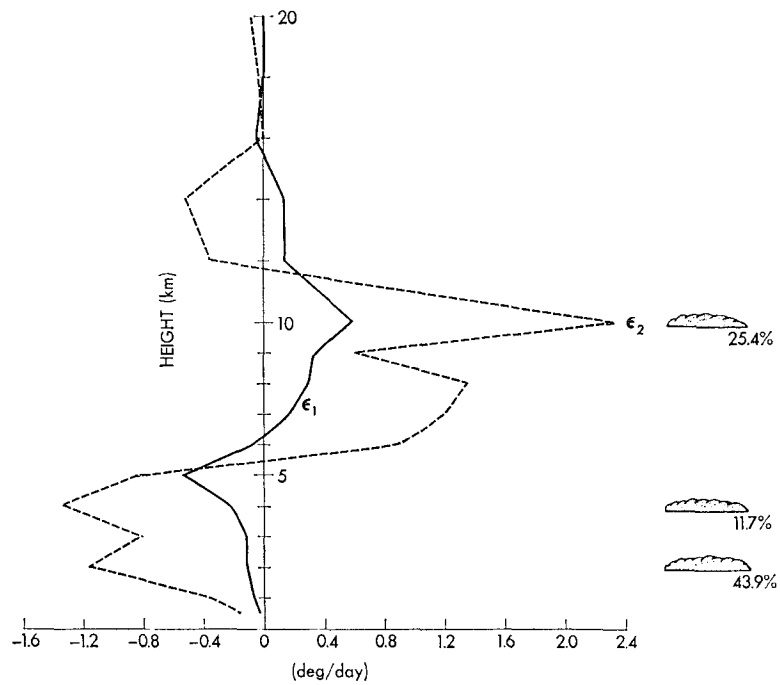

FIG. 6. Errors for the climatological mean approximation with and without the CTS correction. ϵ_1 is the heating rate error using a "climatological average" mixing ratio, and ϵ_2 the error when the CTS correction is applied. The mean and instantaneous mixing ratios used are given in Table 5, Appendix B.

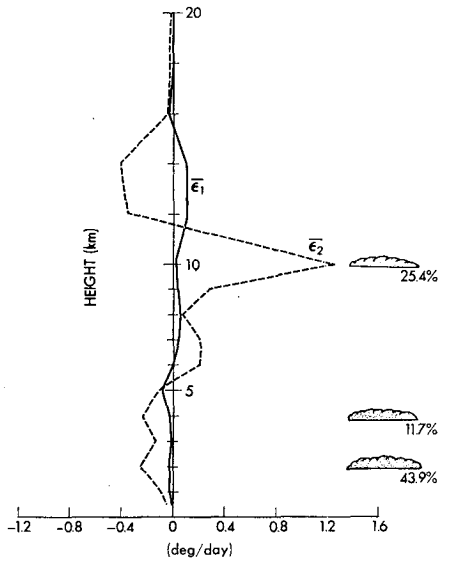

FIG. 7. As in Fig. 6, but averaged over a 5-day period. $\bar{\epsilon}_1$ and $\bar{\epsilon}_2$ are the 5-day means of error curves ϵ_1 and ϵ_2 computed for days 6–10 of the data base. Mean mixing ratios are the same as for Fig. 6.

refer to as $\bar{r}(p)$] was used to calculate an exchange heating rate

$$q_{\text{exchange}}(r) \equiv q(\bar{r}) - q_{\text{CTS}}(\bar{r}).$$

Letting $r(p)$ denote the mixing ratio profile for some given day, our new approximation is just

$$\begin{aligned} q_{\text{approx}}(r) &= q_{\text{exchange}}(\bar{r}) + q_{\text{CTS}}(r) \\ &= q(\bar{r}) - q_{\text{CTS}}(\bar{r}) + q_{\text{CTS}}(r). \end{aligned}$$

In our test, $r(p)$ was any of the profiles for days 6–10 of our 10 day data base.

One set of error curves is shown in Fig. 6. The curve labeled ϵ_1 is the quantity $q(r) - q(\bar{r})$, while ϵ_2 is $q(r) - q_{\text{approx}}(r)$. This particular example was chosen because $\bar{r}(p)$ and $r(p)$ differ greatly, so that ϵ_1 should be large. This is in fact the case, the error reaching the huge value of 2.32 K day^{-1} at 10 km. The use of the CTS correction greatly reduces this value to 0.59 K day^{-1}, but this is still a very substantial error—much larger than any encountered by using the corrected emissivity approximation of Section 3.

For some purposes, the time-mean radiative heating rates may be of more significance than (for example) daily values. (It is important here to distinguish between mean heating rates and heating rates based on mean soundings.) We therefore calculated ϵ_1 and ϵ_2 as defined above for each of the days 6–10 our our data period, and then the time averages $\bar{\epsilon}_1$ and $\bar{\epsilon}_2$. The results are shown in Fig. 7.

Although there has been a not unexpected reduction in ϵ_1 over that of Fig. 6, due to the averaging process, it nevertheless is still large at 10 km. The average error ϵ_2 based on the CTS-corrected approximation, however, is far smaller, never being more than 0.1 K day^{-1}. Several other cases were tested; the results were sufficiently similar to those just presented to require no further discussion.

The potentially great speed of this scheme is degraded substantially in practice by the necessity of allowing for temperature as well as humidity variations. This can be handled by means of a relatively straightforward linearization about some mean temperature profile and does not appreciably affect the accuracy of the method. A more serious problem is presented by variable cloud distribution, for q_{exchange} is very sensitive to this factor. In models which incorporate cloud prediction schemes, use of q_{exchange} based on mean climatological humidities is impractical.

5. Summary and outlook

The approximations discussed may be conveniently arranged in order of ascending accuracy:

1) Cool-to-space (CTS).
2) Use of climatological mean humidity.
3) Climatological humidity with CTS correction.
4) Emissivity.
5) Emissivity with CTS correction.

For all but the crudest purposes the first two are unacceptable, especially in the presence of clouds; the third may be useful for models in which cloud amounts are constant.

Tests under a wide variety of atmospheric conditions show that although emissivity calculations have substantial systematic errors, these are largely eliminated by use of the CTS correction. This leads to a computation scheme which is accurate, efficient and flexible. Not only is the precision of free atmospheric heating rates improved by the use of the CTS correction, but also that of the IR flux at the surface. In situations where even greater accuracy in the evaluation of the ground flux is needed, a "heat from ground" correction may be incorporated.

There are several directions in which this work might be extended. We have completely ignored Doppler broadening of water vapor lines in the present calculation, which is incorrect above 1 mb (Rodgers and Walshaw, 1966). Perhaps use of the Voigt profile in the CTS term alone can adequately account for this effect.

Similarly, CO_2 transmission functions which are precalculated on the basis of a standard temperature sounding cannot incorporate changes in line intensity due to temporal temperature variations. Here, too, it is possible that use of a temperature-corrected CTS term might be of value.

Whether either of these conjectures is correct can only be determined by further work.

Acknowledgments. We would like to thank Drs. L. D. Kaplan, S. Manabe and J. Mahlman, for critically

TABLE 3. Effect of using various temperature corrections in HFG term. The scaled mass is given by

$$dm^* = dm \exp[a(T-260)\times 10^{-3} + b(T-260)\times 10^{-6}],$$

ϵ_2 (high cloud) is the heating rate error at the high cloud layer (K day^{-1}), while ΔF_{ground} is the ground flux error (Wm^{-2}). The first column is the result with no HFG correction. Band number is the infrared band, referred to in the text, corresponding to the values of a and b. The case used is the Trinidad sounding with clouds.

Band no.	—	4	5	6	7	10
a	0.0	9.08	15.1	16.2	18.6	28.5
b	0.0	−38.1	−54.1	−38.1	−62.6	−86.8
ϵ_2 (high cloud)	−0.008	0.027	0.051	0.058	0.065	0.103
ΔF_{ground}	−1.40	− 1.01	− 0.74	− 0.66	− 0.59	− 0.17

reading the first draft of this paper, and for providing useful suggestions. One of us (S. B. F.) benefitted from discussions with Man-Li Wu on the accuracy of the strong-line emissivity and CTS approximations.

Dr. Roland Drayson generously provided the programs which calculate broad-band CO_2 transmission functions from spectral data.

We are grateful to Messrs. P. Tunison and J. Connor for assistance in preparing the figures, and to Miss M. Callan, Mrs. C. Longmuir and Mrs. E. Thompson for their work on the manuscript.

A portion of this work was supported by NOAA Grant 04-3-022-33.

APPENDIX A

Numerical Details

a. Computation of the exchange term.

The use of Eqs. (4) and (5) is complicated in practice by the inclusion of O_3 and CO_2 absorptions, and by the necessity of adequately effecting the vertical quadrature. Random model parameters for water vapor are those of Rodgers and Walshaw (1966) save for their bands 6, 7 and 8, which we took to run from 500 to 560, 560 to 760 and 760 to 800 cm^{-1} respectively. The spectral parameters were recomputed for these intervals using the data of Benedict and Kaplan (1959, and unpublished), as given in Table 5.5 of Goody (1964). With this choice, the 15 μm CO_2 band can be taken to lie entirely in interval 7 with no important error.[8] This greatly simplifies the overlap problem which occurs in that part of the spectrum where both CO_2 and H_2O absorb. In frequency intervals where this is the case, we assume that

$$\tau = \tau_{H_2O}\tau_{CO_2},$$

so that costly evaluation of transmission matrices for water are required. Evidently, if there is only one interval in which overlap occurs, just one such set of τ_{H_2O}'s are required.

The CO_2 transmission functions are pre-computed by a detailed frequency integration of monochromatic functions using a sophisticated program provided by Dr. R. Drayson (Drayson, 1966). The calculation incorporates temperature dependence of line intensities by assuming a mid-latitude standard temperature profile.

The 9.6 μm O_3 band transmission is parameterized by the one-interval random model discussed by Rodgers (1968).

Vertical quadratures are performed using a modified trapezoidal scheme. Denoting the pressure levels at which temperatures are carried by p_j, fluxes are calculated at pressure levels $p_{j+\frac{1}{2}}$, which are halfway between levels p_j and p_{j+1}. The integral which occurs in Eq. (4) of the text is written as

$$\int_0^{p(\text{ground})} \frac{\partial T^4}{\partial p'} G_2[T(p'), u(p', p_{i+\frac{1}{2}})]dp' = \sum_{j=1}^{N} \int_{p_j}^{p_{j+1}} \frac{\partial T^4}{\partial p'} G_2[T(p'), u(p', p_{i+\frac{1}{2}})]dp'.$$

In general, the approximation

$$\int_{p_j}^{p_{j+1}} \frac{\partial T^4}{\partial p'} G_2[T(p'), u(p', p_{i+\frac{1}{2}})]dp' \approx (T^4_{j+1} - T^4_j) G_2[T(p_{j+\frac{1}{2}}), u(p_{j+\frac{1}{2}}, p_{i+\frac{1}{2}})]$$

is used. In calculating the scaled absorber amounts u, mixing ratios are assumed constant throughout each layer.

Due to the rapid variation of G_2 near $u=0$, use of the trapezoidal rule at $j=i$ introduces intolerable errors. For those "nearby layers" the required integral can be expressed in terms of the function $G_3(T,u)$ defined as

$$G_3(T,u) \equiv \int_0^u G_2(T,u')du'.$$

This integral is easy to evaluate and pre-compute. For the frequency interval containing the CO_2 band, a more

[8] Care is required here: If $\bar{\tau}$ is the mean CO_2 transmission for the interval 500–800 cm^{-1}, we use $\bar{\tau}' \equiv 1.5\bar{\tau} - 0.5$ to get the transmission function for the interval 560–760 cm^{-1}. Were there no absorption due to CO_2 outside 560–760 cm^{-1}, this would be rigorously correct. It is also correct when there is CO_2 absorption in the ranges 500–560 and 760–800 cm^{-1}, but no water vapor, as in the upper atmosphere.

TABLE 4. Pressures (mb), temperatures (K) and mixing ratios (10^{-3} kg kg^{-1}) adopted for the 12 cases discussed in Section 3.

Level no.	P	Mean tropical T	Mean tropical r	Mean mid-latitude T	Mean mid-latitude r	Mean polar T	Mean polar r
1	0.0005	180.63	0.002	184.51	0.002	207.8	0.002
2	0.0013	180.63	0.002	184.51	0.002	207.8	0.002
3	0.0033	180.63	0.002	180.65	0.002	207.8	0.002
4	0.0086	180.63	0.002	180.65	0.002	207.8	0.002
5	0.0214	198.15	0.002	196.65	0.002	207.8	0.002
6	0.049	215.65	0.002	216.65	0.002	207.8	0.002
7	0.104	233.15	0.002	236.65	0.002	207.8	0.002
8	0.208	250.65	0.002	254.65	0.002	207.8	0.002
9	0.402	262.15	0.002	264.65	0.002	207.8	0.002
10	0.759	270.15	0.002	270.65	0.002	207.8	0.002
11	1.43	265.75	0.002	265.05	0.002	207.8	0.002
12	2.78	254.75	0.002	251.05	0.002	207.8	0.002
13	5.59	243.75	0.002	237.05	0.002	207.8	0.002
14	11.7	232.75	0.002	226.65	0.002	207.8	0.002
15	15.9	228.35	0.002	224.65	0.002	207.8	0.002
16	21.5	223.95	0.002	222.65	0.002	207.8	0.002
17	29.3	219.55	0.002	220.65	0.002	207.8	0.002
18	40.0	215.15	0.002	218.65	0.002	207.8	0.002
19	54.7	207.15	0.002	216.65	0.002	207.8	0.002
20	75.0	199.15	0.002	216.65	0.002	209.3	0.002
21	102.8	196.50	0.0027	216.65	0.0027	210.6	0.0027
22	141.0	209.90	0.007	216.65	0.007	212.3	0.007
23	193.0	223.30	0.03	216.65	0.02	213.6	0.014
24	264.0	236.72	0.18	223.15	0.058	214.8	0.03
25	307.0	243.44	0.33	229.65	0.12	216.5	0.049
26	356.0	250.17	0.70	236.15	0.22	221.5	0.069
27	410.6	256.94	1.2	242.65	0.42	226.5	0.11
28	471.8	263.71	1.8	249.15	0.66	231.7	0.17
29	540.2	270.54	2.8	255.65	1.0	237.2	0.24
30	616.4	277.36	4.1	262.15	1.5	242.0	0.34
31	701.1	284.28	6.5	268.65	2.4	246.8	0.50
32	795.0	289.34	9.0	275.15	3.4	252.3	0.62
33	898.0	295.89	13.0	281.65	5.0	251.9	0.70
34	954.6	299.24	16.0	284.90	5.7	250.3	0.59
		Trinidad		Washington		Thule	
1		180.6	0.01	184.5	0.005	230.0	0.003
2		180.6	0.01	184.5	0.005	230.0	0.003
3		180.6	0.01	180.6	0.005	230.0	0.003
4		180.6	0.01	180.6	0.005	230.0	0.003
5		198.2	0.01	196.7	0.005	230.0	0.003
6		215.7	0.01	216.7	0.005	230.0	0.003
7		233.2	0.01	236.7	0.005	230.0	0.003
8		250.7	0.01	254.7	0.005	230.0	0.003
9		262.2	0.01	264.7	0.005	230.0	0.003
10		270.2	0.01	270.7	0.005	230.0	0.003
11		265.8	0.01	265.0	0.005	230.0	0.003
12		254.8	0.01	251.0	0.005	230.0	0.003
13		241.0	0.01	237.0	0.005	230.0	0.003
14		229.6	0.0203	226.0	0.0049	230.0	0.003
15		227.1	0.0429	224.8	0.00255	230.0	0.003
16		223.8	0.0727	223.2	0.00116	229.8	0.00326
17		219.1	0.0138	221.2	0.00213	229.5	0.00342
18		212.2	0.00185	220.1	0.00239	227.6	0.00260
19		209.4	0.00298	219.0	0.00232	229.6	0.00290
20		199.6	0.00367	212.8	0.00219	229.3	0.00298
21		194.4	0.00230	216.3	0.00282	229.2	0.00290
22		201.6	0.00695	214.4	0.00271	228.2	0.00283
23		218.0	0.0228	217.4	0.00402	228.2	0.00350
24		232.9	0.103	221.1	0.0209	218.7	0.0455
25		241.5	0.181	228.3	0.125	224.2	0.0788
26		250.7	0.114	236.9	0.382	231.5	0.242
27		256.7	0.053	246.0	0.489	241.3	0.149
28		263.6	0.134	252.4	1.14	245.3	0.402
29		270.5	0.268	258.7	0.862	252.7	0.437
30		277.3	0.633	264.5	2.26	246.9	0.560
31		282.4	1.11	271.5	0.305	253.8	0.982
32		285.7	0.328	275.8	2.53	265.1	1.30
33		290.7	10.2	280.1	2.46	270.2	1.77
34		294.2	21.7	283.4	2.32	274.1	1.87

complicated procedure is required. From the overall transmission

$$\tau(i, i\pm 1)=\tau_{H_2O}(i, i\pm 1)\tau_{CO_2}(i, i\pm 1),$$

a fit to the form

$$\tau(p,p')=\exp(-\alpha|p-p'|^{\frac{1}{2}})$$

is made, which is then integrated analytically as before.

b. Approximation to the HFG correction

The exact heat-from-ground correction is given by Eq. (13). As already pointed out, the additional exact transmission functions required are costly to evaluate. If, however, we make the strong-line approximation, and further assume that the temperature correction factor which scales the absorber amount is independent[9] of n, the band index, then we may make the approximation

$$\sum_n B_n(T)\tau_n(p,p_0)\sim G_2[T,m^*(p,p_0)],$$

where m^* is the temperature and pressure scaled absorber amount.

The choice of the best temperature scaling is somewhat arbitrary, in that improvement in the flux at the ground is accomplished by degradation of cooling rates in the high cloud layer. This is shown in Table 3, where temperature scalings appropriate to various frequency bands are given. On this basis, we decided to use the scaling for band 4 in the computations presented in the text.

APPENDIX B

Data

The pressure, temperature, and humidity data used in the examples of Section 3 are given in Table 4.

In the climatological mean cases, temperatures are based on the *U. S. Standard Atmosphere Supplements 1966* and the humidity below 100 mb on Table A13 of Oort and Rasmusson (1971). Above this level, all mixing ratios are taken to be 2×10^{-6} kg kg^{-1}.

Temperatures and mixing ratios for the three "real data" cases are adapted from Mastenbrook (1966). At a given level, values are taken to be those at the nearest observed data point. The Trinidad case is the 25 March 1965 sounding; Washington that of 13 October 1965. The Thule data is for 1925 GMT 22 August 1965. In these cases, observations were made up to about 10 mb. Above this, mixing ratios are simply taken to be constant and equal to the value at the highest data point, while temperatures are joined smoothly to an appropriate standard atmosphere.

Water vapor mixing ratios used in the tests of Section 4 are shown in Table 5. Data are taken from an 11-layer general circulation experiment whose highest level is at about 20 km, and interpolated linearly to give values at the pressure levels of the radiation model. Above 20 km a constant mixing ratio of 3×10^{-6} kg kg^{-1} is used. Temperatures are those of a mid-latitude standard atmosphere.

[9] By contrast, the emissivity calculation assumes that the temperature correction factor is unity.

TABLE 5. Level heights (km) and mixing ratios (10^{-3} kg kg^{-1}) for the case discussed in Section 3, where $\bar{r}$ is the "climatological mean" mixing ratio, taken as an average of days 1–5 of the time series, and r the mixing ratio for day 10 of the time series.

Level no.	Height	$\bar{r}$	r
19	20	0.00072	0.0012
20	18	0.0016	0.0021
21	16	0.0032	0.0030
22	14	0.0023	0.012
23	12	0.0084	0.031
24	10	0.206	0.127
25	9	0.326	0.184
26	8	0.807	0.152
27	7	1.418	0.094
28	6	2.103	0.030
29	5	3.146	0.324
30	4	4.526	0.939
31	3	6.322	2.081
32	2	9.551	5.517
33	1	15.35	12.34
34	0.5	18.79	17.45

APPENDIX C

The Emissivity Approximation Error

In every curve of ϵ_1 in Figs. 1 and 3 it may be observed that ϵ_1 is positive in the troposphere below about 10 km and negative in the upper atmosphere. The two factors which may produce these errors in the uncorrected emissivity approximation are the use of the strong-line approximation and the neglect of the temperature variations of line intensities.

Our tests [in agreement with Rodgers and Walshaw (1966)] show that errors due to the strong-line approximation are negligible. Errors due to the use of constant line intensities may be understood better by consideration of the factor $d\tau_\nu/dp$ which occurs in the CTS term. [See Eq. (6).] This term may be expressed as $(d\sigma/dp)e^{-\sigma}$, where σ is the optical depth at pressure p for a particular frequency band.

Let σ_e be the optical depth at p for a temperature of 260 K; then one can show that in the upper part of the atmosphere $d\sigma_e/dp>d\sigma/dp$. This is due to the low temperatures in this region and the fact that for the frequencies of importance line intensities decrease with decreasing temperatures.

Near $p=0$, where σ is small, $e^{-\sigma}\sim1$ and $(d\sigma_e/dp)e^{-\sigma_e}>(d\sigma/dp)e^{-\sigma}$, so that the uncorrected emissivity approximation overestimates cooling rates and ϵ_1 becomes negative, as observed in the figures.

As p increases, the fact that $e^{-\sigma_e}<e^{-\sigma}$ grows in importance. Eventually a point must come beyond which $(d\sigma_e/dp)e^{-\sigma_e}<(d\sigma/dp)e^{-\sigma}$. Thus, in the figures, ϵ_1 becomes positive.

If the temperature eventually exceeds 260 K, so that

$$d\sigma_e/dp < d\sigma/dp,$$

as is the case in the tropics and in the middle latitudes, the deviation will be increased; this effect, together with the large amounts of water vapor observed near the surface in low latitudes, accounts for the large values of ϵ_1 observed in Figs. 1 and 3 for these regions.

REFERENCES

Benedict, W. S., and L. D. Kaplan, 1959: Calculation of line widths in H_2O-N_2 collisions. *J. Chem. Phys.*, **30**, 388–399.

Bignell, K. J., 1970: The water-vapour infra-red continuum. *Quart. J. Roy. Meteor. Soc.*, **96**, 390–403.

Cox, S. K., 1973: Infra-red heating calculations with a water vapour pressure broadened continuum. *Quart. J. Roy. Meteor. Soc.*, **99**, 669–679.

Drayson, S. R., 1966: Atmospheric transmission in the CO_2 bands between 12 μ and 18 μ. *Appl. Opt.*, **5**, 385–391.

Elsasser, W. M., 1942: *Heat Transfer by Infrared Radiation in the Atmosphere.* Harvard Meteorological Studies, No. 6, Boston, Harvard University Press.

Feigel'son, E. M., 1970: *Radiant Heat Transfer in a Cloudy Atmosphere.* Leningrad. [Transl. 1973, Jerusalem, Keter Press, 191 pp.]

Fels, S. B., and L. D. Kaplan, 1975: A test of the role of longwave radiative transfer in a general circulation model. *J. Atmos. Sci.*, **32**, 779–789.

Gierasch, P., and R. M. Goody, 1967: An approximate calculation of radiative heating and radiative equilibrium in the Martian atmosphere. *Planet. Space Sci.*, **15**, 1465–1477.

Goody, R. M., 1964: *Atmospheric Radiation.* Oxford University Press, 436 pp.

Manabe, S., and R. F. Strickler, 1964: On the thermal equilibrium of the atmosphere with convective adjustment. *J. Atmos. Sci.*, **21**, 361–385.

Mastenbrook, H. J., 1966: Water vapor observations at low, middle, and high latitudes during 1964 and 1965. Rept. 6447, Naval Res. Lab., Washington, D. C. 206 pp.

Mügge, R., and F. Möller, 1932: Zur Berechnung von Strahlungsströmen und Temperaturänderungen in Atmosphären von beliebigem Aufbau. *Z. Geophys.*, **8**, 53–64.

Oort, A. H., and E. M. Rasmusson, 1971: Atmospheric circulation statistics. NOAA Prof. Paper 5, Govt. Printing Office, Washington, D. C., 323 pp.

Rodgers, C. D., 1967: The use of emissivity in atmospheric radiation calculations. *Quart. J. Roy. Meteor. Soc.*, **93**, 43–54.

——, 1968: Some extensions and applications of the new random model for molecular band transmission. *Quart. J. Roy. Meteor. Soc.*, **94**, 99–102.

——, and C. D. Walshaw, 1966: The computation of infra-red cooling rate in planetary atmospheres. *Quart. J. Roy. Meteor. Soc.*, **92**, 67–92.

Sasamori, T., 1968: The radiative cooling calculation for application to general circulation experiments. *J. Appl. Meteor.*, **7**, 721–729.

——, 1970: Simplification of radiative cooling calculation for application to atmospheric dynamics. *Proc. WMO/IUGG Symposium on Radiation, Including Satellite Techniques.* WMO Tech. Note No. 104, Geneva, 479–488.

Smagorinsky, J., S. Manabe and J. L. Holloway, Jr., 1965: Numerical results from a nine-level general circulation model of the atmosphere. *Mon. Wea. Rev.*, **93**, 727–768.

Yamamoto, G., 1952: On a radiation chart. *Sci. Rept. Tohoku Univ. Ser. 5, Geophys.*, **4**, No. 1, p. 9.